Experimental Investigation and Performance Optimization of the Halo thruster

IEPC-2019-627

Presented at the 36th International Electric Propulsion Conference
University of Vienna • Austria
September 15 –20, 2019

Burak Karadag[1], Silvia Masillo[2], Rachel Moloney[3], Andrea Lucca Fabris[4]
University of Surrey, Guildford, UK

Thomas Potterton[5]
Surrey Satellite Technology Ltd, Guildford, UK

Aaron Knoll[6]
Imperial College London, London, UK

Paolo Bianco[7]
Airbus Defence and Space, Portsmouth, UK

This paper presents an overview of recent experimental research and development activities performed on a Halo thruster permanent-magnets prototype operated on xenon. The thruster performance is assessed for different power levels and mass flow rates. The thrust, measured using a pendulum-type thrust balance, ranges from 5.9 to 12.6 mN for anode discharge powers between 185 and 380 W. The anode specific impulse presents values between 550 and 1100 s and the anode efficiency lies within the 8-25% interval. Anode current traces show strong oscillations at about 15 kHz, suggesting the occurrence of quasi-periodic ionization oscillations similar to the "breathing mode" observed in traditional Hall Effect Thrusters. Finally, plasma emission in the exit plane region is measured at different operating conditions using an optical spectrometer and processed through a collisional-radiative model to infer relevant plasma properties, such as electron temperature.

Nomenclature

Airbus DS	=	Airbus Defence & Space
CHT	=	Cylindrical Hall Thruster
CFT	=	Cusped Field thruster
EP	=	Electric Propulsion
FEMM	=	Finite Element Method Magnetics
HEMPT	=	High Efficiency Multistage Plasma thruster
HET	=	Hall Effect Thruster
ICL	=	Imperial College London

[1] Postdoctoral Research Fellow, Surrey Space Centre, b.karadag@surrey.ac.uk.
[2] Post-Graduate Researcher, Surrey Space Centre, s.masillo@surrey.ac.uk.
[3] Post-Graduate Researcher, Surrey Space Centre, r.moloney@surrey.ac.uk.
[4] Lecturer in Space Propulsion/Electric Propulsion, Surrey Space Centre, a.luccafabris@surrey.ac.uk.
[5] Propulsion Manager, t.potterton@sstl.co.uk.
[6] Senior Lecturer, Department of Aeronautics, a.knoll@imperial.ac.uk.
[7] Project Manager, Global R&T Cooperation, paolo.bianco@airbus.com.

LEO	=	Low Earth Orbit
OES	=	Optical Emission Spectroscopy
PM	=	Permanent Magnet
SSC	=	Surrey Space Centre
SSTL	=	Surrey Satellite Technology Limited
XPT	=	External Discharge Plasma Thruster

I. Introduction

IN the last decades there has been steady growth in the use of Electric Propulsion (EP) in multiple mission profiles such as station keeping in geostationary orbit for telecommunication satellites[1], interplanetary transfers to the Moon (ESA Smart-1 mission[2]) and to Mercury (ESA Bepi Colombo mission[3]), drag compensation (ESA GOCE mission[4]) and constellation phasing[5]. These emerging opportunities have fostered the development of a wide variety of competing electric propulsion technologies encouraging the community to both explore completely disruptive solutions and continue to improve well-established technologies. Hall Effect Thrusters (HETs) have a significant flight heritage and are, at present, the most commonly used Electric Propulsion systems. Challenges are related to the drop of performance if scaled to low power levels typically available on a small satellite (<500 kg and order of ~100-200 W), as a result of increased wall losses and magnetic circuit overheating with decreasing size. Different concepts, such as Cylindrical Hall Thruster (CHT) [6], Cusped Field Thruster (CFT) [7, 8], Quad Confinement Thruster (QCT)[9] and External Discharge Plasma Thruster (XPT)[10] have been developed to mitigate HET scaling issues through alternative magnetic field topologies, discharge channel geometries and propellant injection schemes by increasing the plasma volume-to-area ratio compared to annular HETs in the attempt to reduce wall losses, and improve efficiency at low power.

The Halo thruster has been developed at the Surrey Space Centre (SSC) since 2010 as a novel solution to address the industry need for low cost and low power electric propulsion systems for small satellites. It utilizes a cusped magnetic field configuration with regions of magnetic field cancellation in two locations: a null point at the center of the discharge channel exit, and an annular region in front of the anode from which the thruster acquires its name "halo". The rationale behind this magnetic topology is fostering the increase of electron confinement, reduction of wall losses, decrease of the beam divergence, as well as enabling advanced engineering solutions such as the use of a centrally located cathode and the use of permanent magnets. The main components of the thruster are a ceramic channel, an anode, a hollow cathode neutralizer and an applied magnetic field, generated either by permanent magnets and electromagnets (Figure 1). The hollow cathode neutralizer produces a stream of electrons to sustain the plasma within the discharge channel and to neutralize the ejected ion beam. Within the discharge channel, electrons are trapped in closed azimuthal drifts, resulting from the combination of electric and magnetic field, impeding the local electron axial transport. This effect establishes a strong local electric field that accelerates the ions away from the thruster with high exhaust velocity, similarly to the acceleration mechanism in traditional Hall Effect Thrusters.

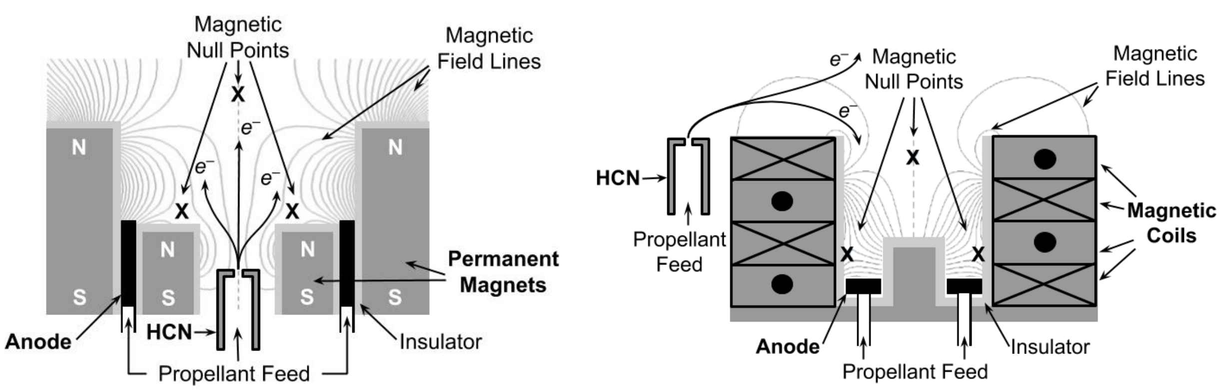

Figure 1. General schematics of the Halo Thruster and its main components. On the left: permanent magnets configuration with centrally-located cathode. On the right: electromagnets configuration.

SSC is carrying out the experimental development of this new technology in collaboration with Airbus Defence & Space (ADS), Surrey Satellite Technology Limited (SSTL) and Imperial College London (ICL). Different prototypes have been tested with different geometries, magnetic field solutions (permanent magnets or electromagnets), hollow cathode configurations and propellants. This paper presents an overview of the research activities on the permanent magnet version of the Halo thruster prototype, including preliminary performance measurements, optical emission spectroscopy data and the assessment of plasma oscillatory modes under certain operating conditions. Experimental characterizations of the Halo Thruster variants with electromagnets can be found in previous publications[11, 12].

II. Permanent Magnet Halo Thruster

A cutaway view of the permanent magnet (PM) Halo thruster CAD model showing all of the main components of the thruster is given in Figure 2. Two ceramic parts enclose the cylindrical discharge channel. The copper anode with an annular internal cavity serves as the positive electrode, drawing electron current from the plasma, but it also functions as the propellant gas distributor. The anode should provide an azimuthally uniform neutral gas flow as azimuthal non-uniformity or heterogeneity of the propellant density might reduce thrust efficiency[13, 14] and besides, the injection should decrease the axial speed of the gas flow increasing residence time of neutrals in the discharge channel to achieve higher propellant ionization. In the PM Halo thruster, the anode and a ceramic part protecting the inner magnet are coaxially placed to form a deep annular channel providing more uniform azimuthal propellant flow compared to using a set of equally spaced holes. The anode sits at the outer edge of the discharge channel. The propellant gas is fed radially from an inlet within the annular section of the thruster on the outer discharge channel wall, and flows around the anode to enter the discharge channel. The thruster features a cavity along the symmetry axis of the thruster so that an electron source or ion beam neutralizer can be placed. A copper heat sink, with optional water cooling, is employed at the rear of the thruster, intended to prevent overheating of the magnets during extended operation. The component labeled as “central electrode”, made of molybdenum, prevent the propellant back flowing, and serves as an auxiliary electrode.

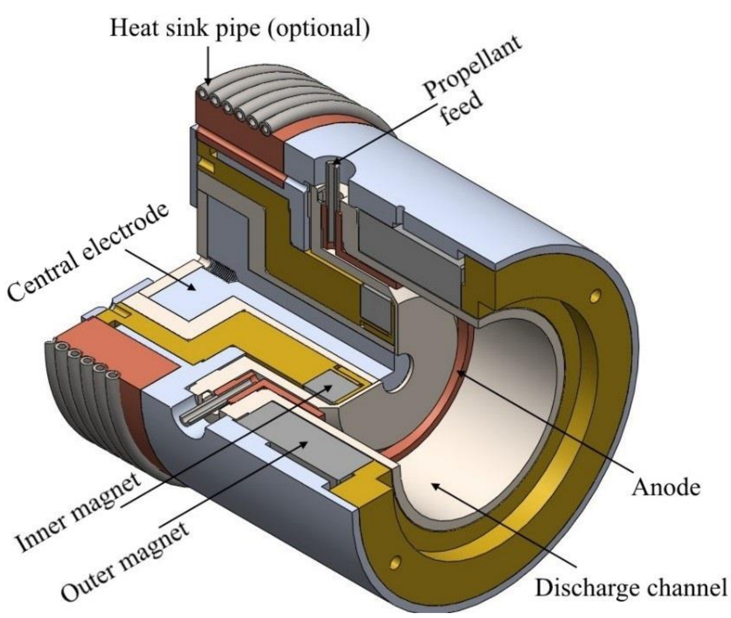

Figure 2. A cutaway view of the PM Halo thruster 3D CAD model.

The use of permanent magnets in electric thrusters presents a growing trend[15-16, 10] due to various advantages. Permanent magnets enable high magnetic field strengths at small scale providing better plasma confinement, reducing wall sputtering erosion caused by high-energy ions and decreasing power loss associated to plasma losses to the channel walls. They also circumvent the excessive heat dissipation issue of coils, and simplify the thruster design as there is no need for additional electrical power and associated power supplies. On the other hand, magnets might be considered not favorable from a spacecraft integration perspective because of both the constant residual magnetic dipole needing compensation in order to avoid generating a torque in LEO missions (due to interaction with the Earth magnetic field) and because of magnetic compatibility with other on board equipment that needs to be ensured.

The magnets installed in the Halo assembly are made of samarium cobalt (SmCo) and are enclosed in metal cases connected to the thruster body using threads. SmCo magnet was selected for its strong maximum energy density product (BH), strong resistance to demagnetization (coercivity) and high working temperature. The PM Halo thruster embeds two concentrically aligned samarium cobalt hollow cylindrical permanent magnets of grade XG24/25 with a maximum energy product of 24 Mega Gauss Oersteds (MGOe) and a working temperature of 350 °C. The alignment of the permanent magnets with like poles facing in the same direction results in four axisymmetric cusp regions within the thruster discharge channel and an annular magnetic cancellation region near the anode. Figure 3(a) shows magnetic flux density of the magnetic circuit simulated by Finite Element Method Magnetics (FEMM) [17]. The figure highlights an annular magnetic field cancellation region within the discharge channel enclosed by a toroidal cusp structure along with a spherical magnetic field cancellation region, which is also enclosed by a cusp structure, along the thruster axis of symmetry downstream the thruster exit. The internal toroidal magnetic null region is called "halo" giving the thruster its name, while the external spherical magnetic null region is labeled as "null point".

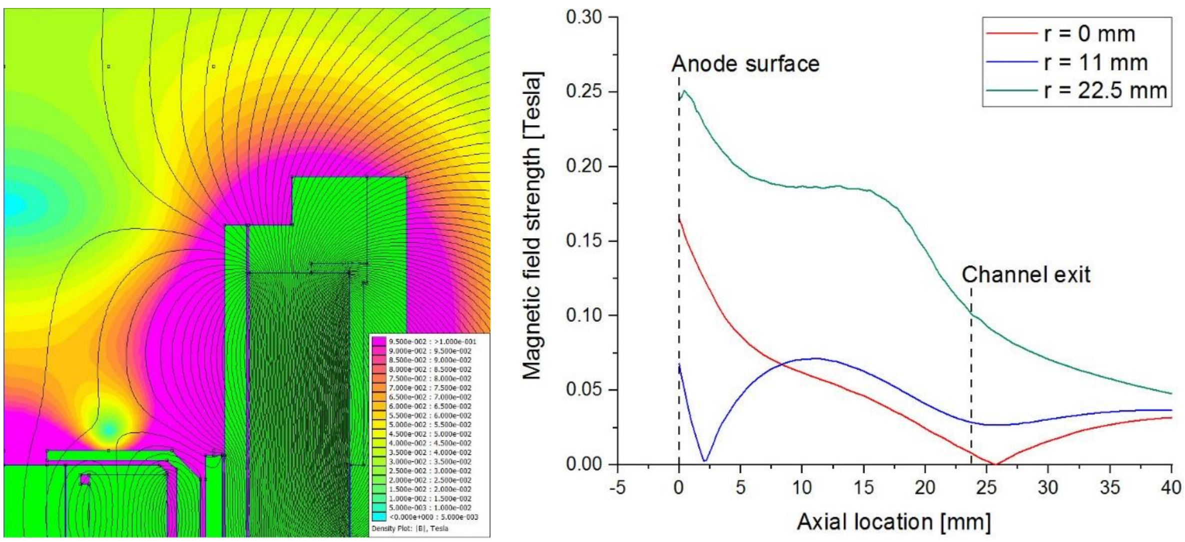

a) Magnetic flux density distribution.

b) Total magnetic field strength profile along the central axis, along an axial path through the halo null region and along an axial path from the anode.

Figure 3. Magnetic circuit model calculated by FEMM.

Figure 3(b) compares the total magnetic field strength of the PM Halo thruster along the symmetry axis (r = 0 mm), an axial path partially intersecting the halo (r = 11 mm) and an axial path starting from the anode downstream surface (r = 22.5 mm), which corresponds to the red, blue and green lines respectively in Figure 3. The halo is visible in the blue line, while the null point is visible in the red line. The halo is located at approximately 5 mm in front of the inner magnet. The magnetic field strength is quite large especially along the discharge channel walls where it peaks at above 0.3 Tesla.

III. Experimental Setup

A. Vacuum Facility

The experimental campaigns described in this paper were carried out in the Daedalus test facility at the Surrey Space Centre Electric Propulsion Laboratory. The Daedalus facility consists of a vacuum chamber measuring 1.5 m in diameter and 3 m in length, with a three-stage pumping system incorporating two cryogenic pumps in parallel with a turbomolecular pump. The chamber achieves a base pressure in the range of 10^{-6} Torr. The chamber is equipped with a variety of feedthroughs and propellant feedlines, thruster power lines, sensor signal lines and a series of viewing ports at different locations around the chamber. Multiple pressure gauges are installed in critical locations along the vacuum system to measure pressure levels in the chamber and pumping lines.

B. Direct Thrust Measurement

A hanging pendulum-type thrust stand with sub-milliNewton resolution developed at SSC was used to take direct thrust measurements. The thrust stand assembly is made of a movable platform attached to a rigid support structure via four thin flexures. The thruster is interfaced to this platform, and the displacement of the platform from the zero position due to the generated thrust is measured through a laser sensor (Micro-Epsilon model ILD 1700-2). The thruster is electrically isolated from the thrust stand through ceramic bushes inserted between the mounting bolts of the thruster and the interface plate.

The measured displacement of the platform depends on the thrust according to a linear relationship, whose slope (i.e. the calibration factor) is determined using an embedded calibration system, which consists of a movable mass moved by a rotational stage with pulley system producing a variable force acting on the platform. Typically, ten force values are used for each calibration. The calibration process is performed in vacuum conditions with feedlines and power lines already installed to include their inherent stiffness in the resulting calibration factor. The displacement data are processed using a Matlab code, which applies 5th order low-pass filter to the raw data, automatically identifies the displacement steps and performs a linear interpolation of the thrust values versus the displacement to compute the calibration factor. A Monte Carlo algorithm is used to quantify the uncertainty of the calibration factor originating from the uncertainties of mass and geometrical dimensions. The calibration is repeated three times and the average is taken for thrust calculations. When the thruster firing is ceased, the platform displacement experiences a step-change. The magnitude of the displacement step, corresponding to the force that the thruster generates, is calculated through a linear interpolation of the readout before and after the thruster was switched off by using a Python code. The thrust is then obtained by multiplying calibration factor and displacement value.

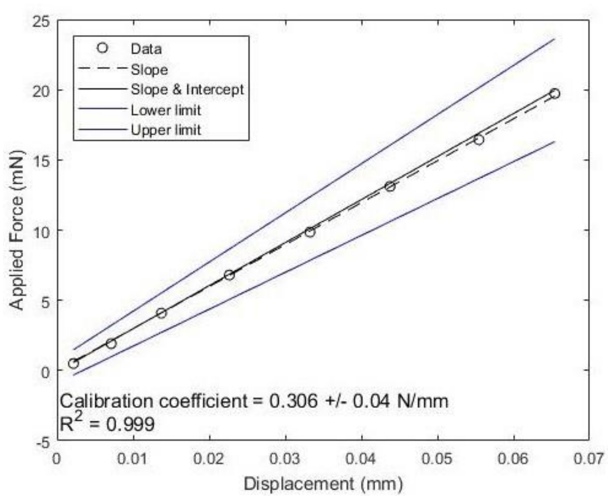

a) Calibration curve.

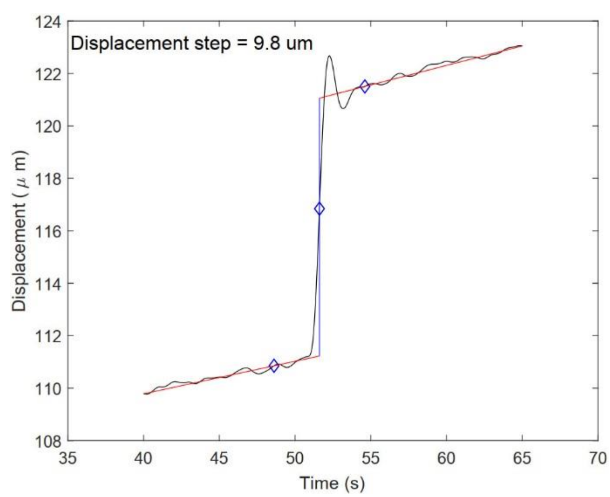

b) Displacement time series.

Figure 4. An example of calibration curve output and displacement step calculation.

An example of calibration curve output by the Matlab code, including the upper and lower limits resulting from the uncertainty analysis, is shown in Fig. 4 (a). An example of displacement step calculation output by the Python code is shown in Fig. 4(b). During this experimental campaign, the thrust measurement at each operating condition was repeated three times; the plots in the following sections report the mean as the central point and the standard deviation in form of double-sided error bar.

C. Optical Emission Spectroscopy (OES)

Optical emission spectroscopy (OES) provides a rapid means of gaining insight into plasma properties such as local electron temperature. Light emitted from the plasma plume is collimated through a lens (Ocean optics 74-series) placed perpendicular to the thruster symmetry axis downstream the thruster exit. The intensity of the emission spectrum is detected by a spectrometer (Ocean Optics HR4000CG-UV-NIR) using an integration time of 0.5 s. Space-averaged electron temperatures (T_e) is estimated using intensity ratio of xenon 823 nm and 828 nm lines according to the collisional radiative model presented by Dressler et al.[18]. Figure 5(a) shows the experimental setup, and Fig. 5(b) plots the 823/828 nm line intensity ratios as a function of electron temperature for a Hall thruster with an acceleration voltage of 300 V at which ion collision excitation cross sections have smooth variation, and doubly charged ion signals are significantly weaker.

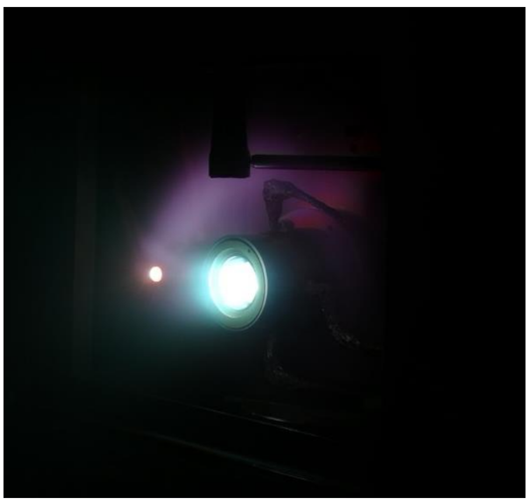

a) OES experimental: the collection lens is the dark shadow over the thruster plume.

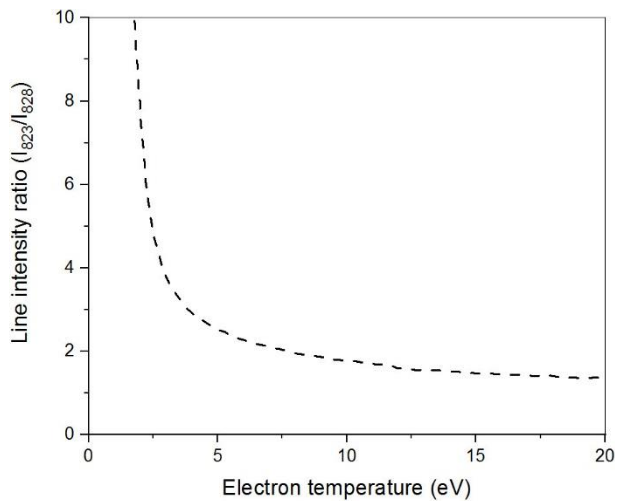

b) Line intensity ratio as a function against electron temperature

Figure 5. OES experimental setup and line intensity ratio plot from the collisional radiative model in Ref. 18.

D. Operating Conditions

For the experimental campaign described in this paper, the hollow cathode neutralizer was mounted externally to the thruster at an angle of 45° with respect to the thruster axis with the cathode orifice approximately 100 mm away from the thruster centerline. Both cathode and thruster head were electrically isolated from vacuum chamber ground, and floated during the measurements. The central electrode was either floated or grounded to examine its effects on the thrust performance. High purity xenon gas was used as propellant for both the anode and the hollow cathode. The cathode mass flow rate (0.29 mg/s), cathode heater current, and cathode keeper current were kept constant. The anode potential and mass flow rate were 200-250-300 V and 0.98-1.08-1.18 mg/s, respectively. The propellant mass flow was regulated using xenon mass flow controllers (Bronkhorst model F-201CV-020-AAD 22-V, 10 sccm full range, calibrated by the manufacturer) with a maximum uncertainty of 0.002 mg/s.

A high frequency current probe (Hioki 3273-50) with a bandwidth of 50 MHz was attached to the anode power line near the high voltage power supply to record discharge current waveforms. There was not any filter unit between the thruster and the power supply. Background pressure was measured by an ion gauge (Edwards AIM-S-NW25) located on right hand side of the vacuum chamber, and corrected for xenon. Background pressure was maximum 1.3×10^{-4} Torr at 1.18 mg/s anode mass flow rate and 0.29 mg/s cathode mass flow rate.

IV. Results and Discussion

A. Visual Observations

Figure 6 shows front and side views of the PM Halo thruster during operation at 1 mg/s xenon mass flow rate and 300 V anode potential with the central electrode floating. It can be seen that plasma density is concentrated along the discharge channel centerline near the internal magnetic null region (Halo) expanding axially towards the external magnetic null region (Null point) at the thruster exit plane. A clear offset of the plasma from the discharge channel side wall is seen where the magnetic field lines are parallel to the wall surface similar to a magnetically shielded Hall thruster[19]. Visual observations of the discharge plasma suggest that total volumetric erosion rate of the discharge channel may be lower compared to a conventional Hall thruster. However, the wall sheath potential structure should be investigated for further evidence. Therefore, numerical simulation of the Halo thruster discharge by a fully kinetic PIC-DSMC code[20] will be our future work.

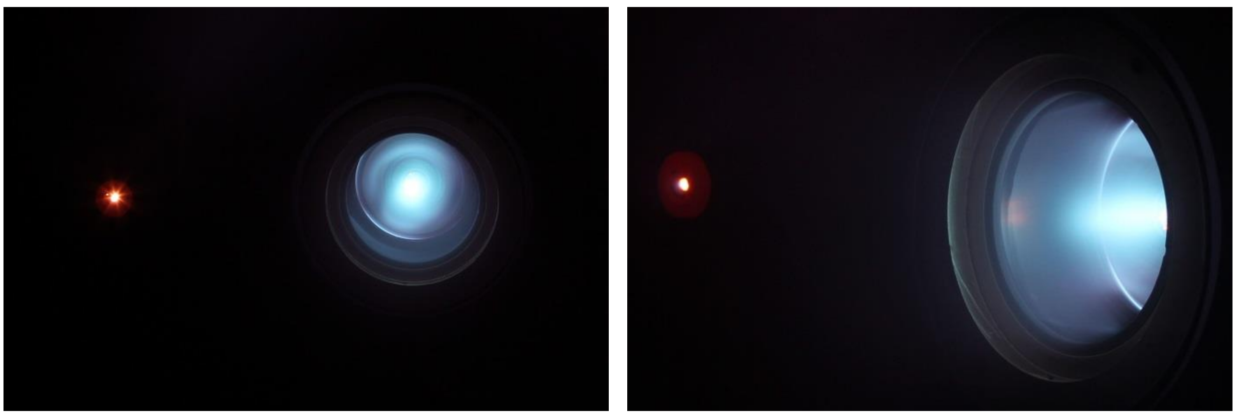

Figure 6. The PM Halo thruster discharge front view (left) and side view (right). *The cathode was mounted parallel to the thruster axis.*

B. Thruster Performance

The discharge current as a function of the anode potential is shown in Fig. 7 (a). The discharge current increases slightly (1-3%) for the grounded central electrode configuration compared to the floating central electrode one. In the latter configuration, the floating potential of the central electrode varied between 30-36 V. This potential barrier is removed when the central electrode is grounded, potentially leading more ions to strike on the central electrode surface increasing secondary electron emission (SEE) to the bulk plasma in the discharge channel.

Thrust versus anode potential is shown in Fig. 7 (b). The thrust monotonically increases with discharge voltage and anode mass flow rate. The average thrust values for the floating central electrode configuration ranged from 5.9 to 12.6 mN at discharge powers of 185 to 380 W translating to anode efficiencies of 8-25%. The thrust presents a sensible decrease (up to 25%) when the central electrode is grounded. This difference is too large to be explained with the 1-3% increase in the discharge current. The cathode-to-ground voltage varied between -28 to -32 V, and there was no significant difference between both configurations. A possible explanation originates from the different plasma potential distribution in the discharge channel with a decrease of the axial electric field. Increased secondary electron emission may lower the total electron temperature in the discharge channel, enhance the cross-field electron transport by modifying the sheath potential[21], and limit the maximum achievable electric field in the magnetized plasma[22].

The anode specific impulse as a function of the anode potential is shown in Fig. 7 (c) and the thrust versus the average discharge power is shown in Fig. 7 (d). The anode specific impulse increases with increasing discharge voltage as expected. Anode specific impulses of 558 to 1088 s and thrust-to-power ratios of 23 to 45 mN/kW were achieved across the operating conditions. Fig. 7 (c) and (d) also compare the performance of the PM Halo thruster to the EM Halo thruster with 5-cm channel diameter[11, 12]. The permanent magnet version reaches higher thrust-to-power ratios, while the electromagnetic coil version provides higher anode specific impulses. It can be said that the EM Halo thruster has better propellant utilization efficiency or “ionization efficiency” due to the short annular part in its discharge channel, yielding to increased neutral density and ionization probability. The PM Halo thruster can be said to have better “acceleration efficiency” due to its stronger magnetic field as the total thrust is proportional to Hall current and magnetic field ($T \propto j \times B$).

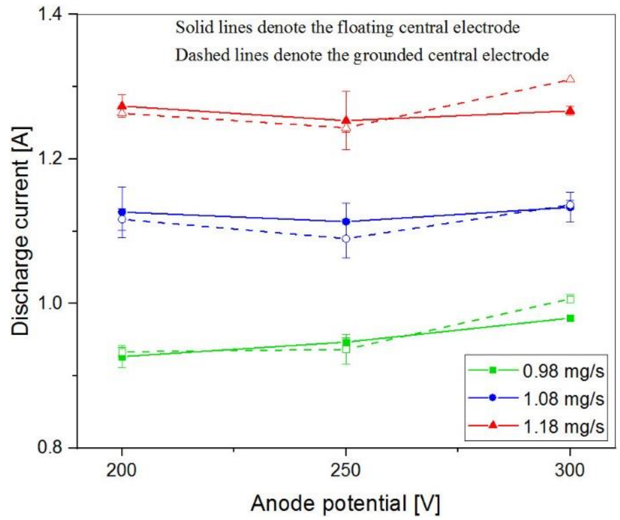

a) Discharge current against anode potential

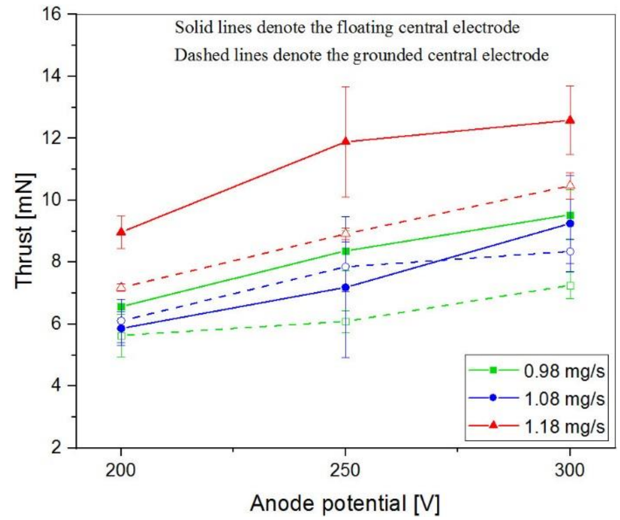

b) Thrust against anode potential

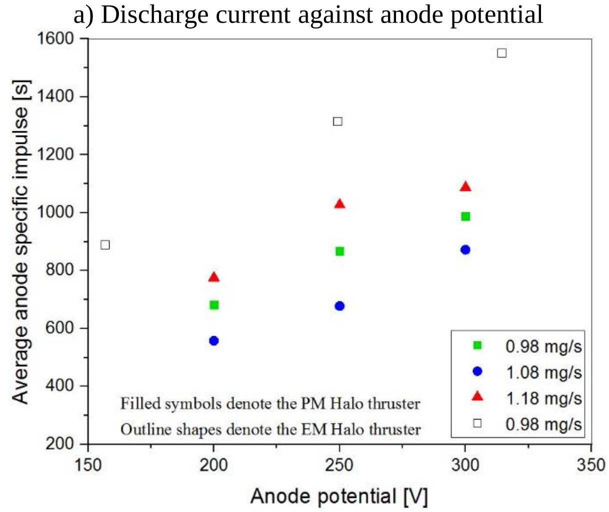

c) Anode specific impulse against anode potential

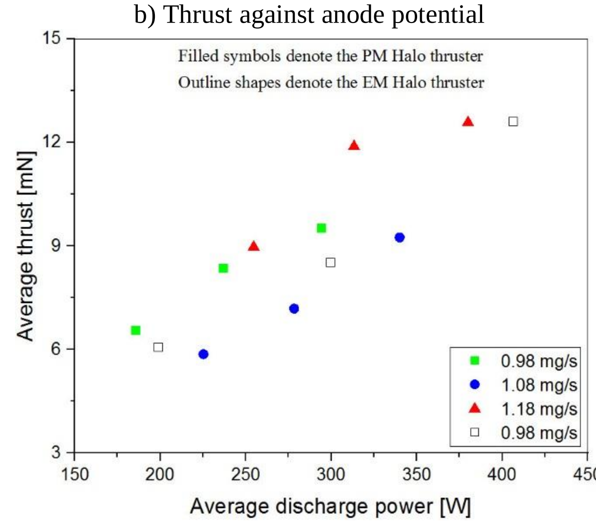

d) Thrust-to-power ratio

Figure 7: Thrust performance results. *The electromagnetic coil current and cathode mass flow rate for the EM Halo thruster[10] were 2 A and 0.2 mg/s respectively.*

C. Discharge Current Waveforms

Figure 8 shows discharge current waveforms for 0.98 mg/s and 1.18 mg/s mass flow rate conditions. Low frequency discharge current oscillations (5-35 kHz) are related to ionization processes, and correspond to the so-called breathing mode[23]. The PM Halo thruster shows breathing mode oscillations with peak-to-peak current as large as 6 A. The period of the waveforms is comparable to the neutral residence time of xenon atoms in the discharge channel, which is around 70 µs at an anode/wall temperature of 700 K. The oscillation amplitude increases when the anode potential is increased from 200 V to 300 V. The increase of the oscillation amplitude due to increased anode potential is more severe for the 1.18 mg/s anode mass flow rate condition compared to 0.98 mg/s.

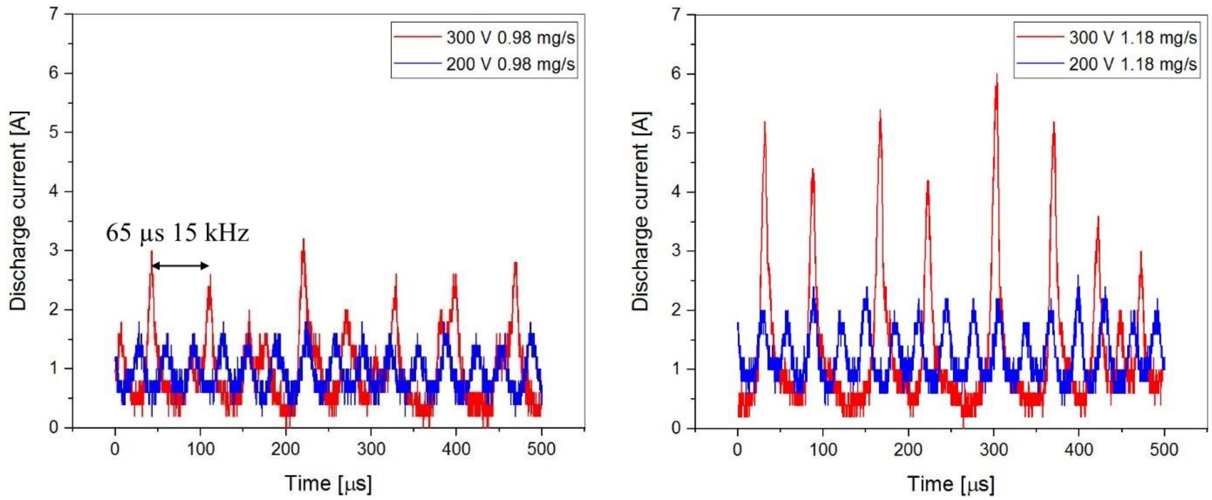

Figure 8. Discharge current waveforms for 0.98 mg/s and 1.18 mg/s mass flow rate conditions.

D. Emission Spectra

The optical emission spectra present the same pattern for all the operating conditions. The emission spectra obtained for 200-300V anode voltages and 0.98 mg/s mass flow rate condition is shown in Figure 9. The intensity of the 823/828 nm and 895/915/904 nm lines decreases with increasing anode potential, while the intensity of the 461-543 nm lines increases with increasing anode potential. This can be associated to higher ionization due to the increased electron temperature; indeed, emission lines for xenon neutral (Xe I) and xenon single ion (Xe II) are prominent in the 800-900nm and 400-600nm wavelength regions respectively. The previously mentioned collisional radiative model using 823 nm and 828 nm line intensity ratios (I823/I828) suggests an average electron temperature of 2-3 eV at the near-exit plume.

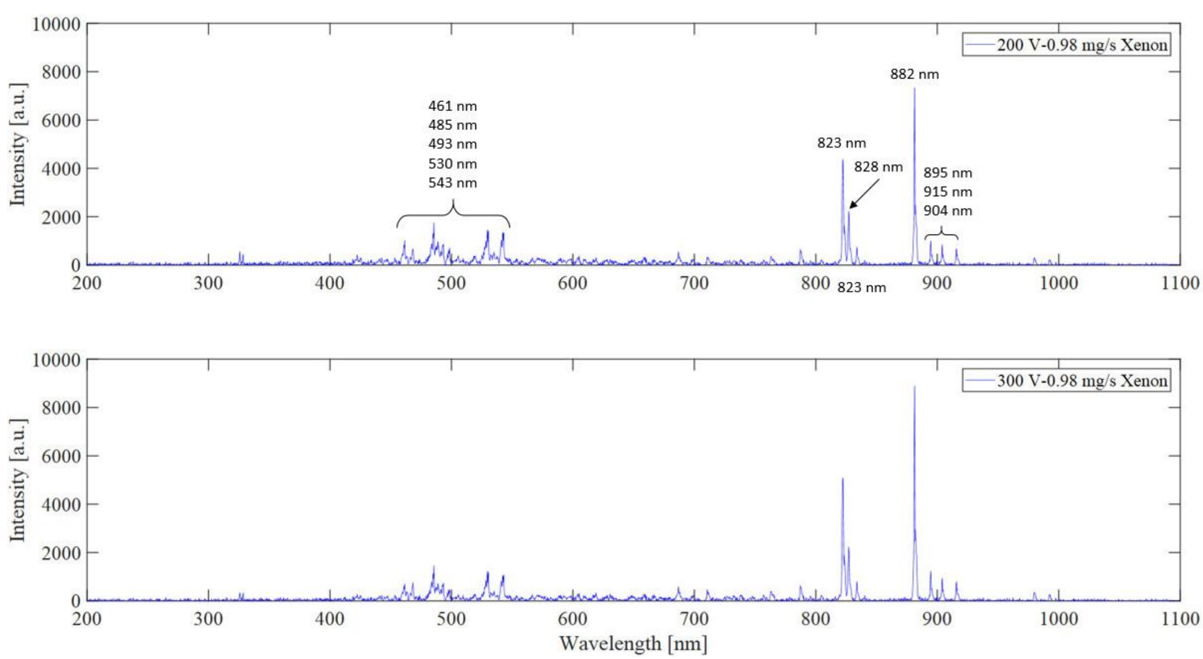

Figure 9. Comparison of the plume emission spectra for 200 and 300 V discharge voltages.

V. Conclusion

The Halo Thruster is a novel propulsion concept based on the electrostatic acceleration of propellant ions produced in a DC-powered magnetised plasma discharge characterized by a closed-loop electron drift sustained by the combination of electric and magnetic fields. The magnetic field structure of the Halo thruster was designed to include magnetic null regions: a downstream null point near the channel exit and an upstream annulus in front of the anode.

Recent experimental research activities have characterized the performance of a 5 cm diameter Halo thruster permanent-magnets prototype operated on xenon. The experimental setup included a pendulum-type thrust balance for direct thrust measurements, an optical spectrometer to monitor plasma emission in the exit plane region and a high-frequency current probe to detect anode current fluctuations.

The thruster have been operated between 185 W and 380 W, producing a thrust between 5.9 and 12.6 mN. The anode specific impulse presents values between 550 and 1100 s and the anode efficiency lies within the 8-25% interval. Comparisons with previous data derived on a similar Halo thruster prototype based on electromagnets[11, 12] suggest that the permanent magnet version reaches a higher thrust-to-power ratio, while the electromagnetic coil version provides a higher anode specific impulse. This performance offset might depend on the magnetic fields of the prototypes that present differences in terms of both strength and topological features, as well as different configurations (e.g. anode size and location) of the discharge channels.

Anode current traces show strong oscillations at about 15 kHz, a value that is compatible with ionization oscillations previously observed in traditional Hall Effect Thrusters. Finally, the processing of plasma emission using a collisional-radiative model estimates an electron temperature of 2-3 eV in the near-field plume.

Acknowledgments

The Halo thruster research and development activities are supported by Airbus Defence & Space and the UK Space Agency under the “Development of a Halo-200 Electric Propulsion System” project.

References

[1] J.J. Delgado, J. A. Baldwin, R. L. Corey. "Space systems Loral electric propulsion subsystem: 10 years of on-orbit operation." 34th International Electric Propulsion Conference, Kobe-Hyogo, Japan, 2015. IEPC-2015-04.

[2] C.R. Koppel, D. Estublier. "The SMART-1 Hall effect thruster around the moon: In flight experience." 29th International Electric Propulsion Conference, Princeton, USA, 2005. IEPC-2005-119.

[3] M. Hutchins, H. Simpson, J. Palencia Jiménez. "QinetiQ’s T6 and T5 Ion Thruster Electric Propulsion System Architectures and Performances." 34th International Electric Propulsion Conference, Kobe-Hyogo, Japan, 2015. IEPC-2015-131.

[4] N. Wallace, P. Jameson, C. Saunders, M. Fehringer, C. Edwards, R. Floberghagen. “The GOCE ion propulsion assembly-lessons learnt from the first 22 months of flight operations”. 32nd International Electric Propulsion Conference, Wiesbaden, Germany, 2011. IEPC-2011-327.

[5] S. Oleson, J.M Sankovic, “Electric Propulsion for Low Earth Orbit Constellations”. 1998 JANNAF Propulsion Meeting, Cleveland, Ohio. 1998.

[6] Y. Raitses, N.J. Fisch. “Parametric Investigations of a Nonconventional Hall Thruster”. Physics of Plasmas, 8(5), 2579-2586.

[7] N. Koch, H.P. Harmann, G. Kornfeld. “Development and Test Status of the THALES High Efficiency Multistage Plasma (HEMP) Thruster Family”. 29th International Electric Propulsion Conference, Princeton, USA, 2005. IEPC-2005-297.

[8] D.G. Courtney. “Development and Characterization of a Diverging Cusped Field Thruster and a Lanthanum Hexaboride Hollow Cathode”. MSc Thesis, Massachusetts Institute of Technology.

[9] A.K. Knoll, T. Harle, V. Lappas, and M. Pollard. “Experimental Performance Characterization of a Two-Hundred-Watt Quad Confinement Thruster,” Journal of Propulsion and Power, 30(6) 1445-1449, 2014.

[10] B. Karadag, S. Cho, I. Funaki, Y. Hamada, and K. Komurasaki, “External discharge plasma thruster,” J. Propul. Power. 2018.

[11] T.G. Wantock. “Thrust Balance Performance Characterisation and Internal Langmuir Probe Plasma Diagnostics for a Halo Thruster”. PhD Dissertation, University of Surrey, UK. 2017.

[12] A. Lucca Fabris, T. Wantock, A. Gurciullo, R. Moloney, A. Knoll, T. Potterton, P. Bianco. “Overview of Halo thruster research and development activities”. Space Propulsion Conference Proceedings. 2018.

[13] V. Baranov, Y. Nazarenko, V. Petrosov, “Azimuthal non-uniformities in accelerators with closed electron drift.” 27th International Propulsion Conference, Pasadena, USA, 2001. IEPC-01-18.31F.

[14] Yasuhiro, S. Yokota, K. Komurasaki, Y. Arakawa, “Oscillation reduction of an anode-layer-type Hall thruster by azimuthal propellant non-uniformity,” AIAA Paper 2008-5187, 2008.

[15] T. Ito, N. Gascon, W.S. Crawford, M.A. Cappelli, “Further Development of a Micro Hall Thruster”. 42nd Joint Propulsion Conference, Sacramento, USA, 2006. AIAA-2006-4495.

[16] V. Khayms, M. Martinez-Sanchez, “Fifty-Watt Hall Thruster for Microsatellites,” Micropropulsion for Small Spacecraft, Progress in Aeronautics and Astronautics, Vol. 187, AIAA, 2000, pp. 233-254
[17] D. C. Meeker, Finite Element Method Magnetics: Version 4.2(2010); software available at www.femm.info.
[18] Dressler, R. A., Y. Chiu, O. Zatsarinny, K. Bartschat, R. Srivastava, L. Sharma. “Near-Infrared Collisional Radiative Model for Xe plasma electro-static thrusters: the role of metastable atoms”. Journal of Physics D: Applied Physics, 42, 2009.
[19] I. Mikellides, I. Katz, R. Hofer, D. Goebel, K. de Grys, A. Mathers, “Magnetic shielding of the channel walls in a Hall plasma accelerator,” Phys. Plasmas, vol. 18, no. 3, p. 033501, 2011.
[20] B. Karadag, S. Cho, I. Funaki, “Sensitivity Analysis of a Fully Kinetic Code for Physical Parameters,” Journal of the Japan Society for Aeronautical and Space Sciences, Vol. 60, No. 2, p.67-76, 2017.
[21] A.I. Morozov, V.V. Savelyev, “Fundamentals of Stationary Plasma Thruster Theory”, Review of Plasma Physics, Vol. 21. (Edited by B.B. Kadomtsev and V.D. Shafranov), Consultant Bureau, New York, 2000.
[22] Y. Raitses, I.D. Kaganovich, A. Khrabrov, D. Sydorenko, N. J. Fisch, A. Smolyakov, “Effect of Secondary Electron Emission on Electron Cross-Field Current in E×B Discharges”, IEEE Trans. Plasma Sci. 39, 995-1006, 2011.
[23] Boeuf J. P., Garrigues L., “Low frequency oscillations in a stationary plasma thruster,” J. Appl. Phys. 84, 3541, 1998.